Sail aerodynamics

Sail Aerodynamics: On-Water Pressure Measurements on a Downwind Sail

Author Names: Ignazio Maria Viola, ***Member***
Richard G J Flay

ABSTRACT

Pressures on three horizontal sections of a downwind sail were measured for several wind directions and sail trims. The pressure distributions were compared with wind tunnel tests: similarities and differences were found, the latter due to the dynamic effects, which were not modelled in the wind tunnel. A pressure distribution at the head of the spinnaker resembling that from a delta wing was measured at an apparent wind angle of 120°.

KEY WORDS: Sail Aerodynamics; Downwind Sail; Asymmetric Spinnaker; Pressure Measurements; Full-Scale Tests; Model-Scale Tests; Wind Tunnel Tests.

INTRODUCTION

Sail aerodynamics has been widely investigated in the last century. Sails made from different materials and made in different shapes have been compared with full-scale tests, wind tunnel tests and numerical computations. These three approaches allow different aspects of sail aerodynamics to be investigated. Unfortunately, each of them has some limitations, and none of them are able to substitute for the other two. The present paper investigates sail aerodynamics in downwind sailing conditions from on-water tests.

Computational Fluid Dynamics

In the past few decades, numerical programs have become the most commonly used research tool for sails. In the 1960s, potential-flow computational methods were used for 2D horizontal sail sections. In the following years, the fast growth of computational resources led to Navier-Stokes solvers being used more and more frequently. Sails behave very differently in upwind and downwind conditions. A yacht sails upwind or downwind when the supplementary angle (called the true wind angle TWA) between the wind velocity and the yacht velocity is lower or higher than 90°, respectively. Nowadays, while potential-flow solvers are widely used for upwind sailing conditions, Navier-Stokes programs are most commonly used for downwind conditions. In fact, in upwind sailing conditions, the sails are expected to often operate near the maximum lift/drag ratio where the flow would have an attached boundary layer on most of the sail surface. Potential-flow codes, which are unable to model separated boundary layers, can compute aerodynamic forces with a reasonable accuracy in upwind conditions. Conversely, in downwind sailing conditions, sails are designed to operate nearer the maximum lift and, therefore, they have more cambered sections and higher pressure gradients. The boundary layer separates before the trailing edge over a large part of the sail surface due to the high adverse pressure gradients. To correctly compute the aerodynamic forces, separation has to be computed correctly by modelling the effects of viscosity of the fluid. Therefore, Navier-Stokes computational fluid dynamic programs are most commonly used to model downwind sail aerodynamics.

Due to the relatively high sail Reynolds number, at the present time direct Navier-Stokes computations cannot be used in sail aerodynamics, even when very large computational resources are available (Viola & Ponzini, 2011). Therefore, Reynolds Averaged Navier-Stokes (RANS), Large Eddy Simulations (LES) or Detached Eddy Simulations (DES) techniques have to be used to model the small-scale turbulence neglected by the limited grid resolution. These techniques use based on heuristic equations, which need to be validated with experimental measurements. Validations should be repeated every time the modelled geometry or the fluid characteristics are changed significantly. Wind-tunnel tests can be performed for this purpose.

Wind Tunnel Tests

Wind tunnel tests allow the designer to have a real-time aerial view of the flying sails. Smoke visualization or other similar techniques allow streaklines to be visualised very efficiently. At the Yacht Research Unit of the University of Auckland, forces are measured with a 6-component balance located below the wind tunnel floor. It is common practice to use flexible sails, which can be trimmed remotely. Therefore, the change of forces and streaklines with change in the sail trim can be appreciated immediately. In most of the wind tunnels where sail aerodynamics is investigated, special devices allow the flying shapes to be detected. Thus the aerodynamic forces and flying shapes are recorded simultaneously. This increases the repeatability of the measurements and allows differences between sails and trims to be better appreciated. It also allows flying shapes to be modelled with numerical solvers, and computed forces to be compared with measured forces. However, validating numerical simulations just with forces is not ideal. In fact, the pressure distribution on sails might well be computed incorrectly even when the computed resultant aerodynamic forces agree with the measured forces. This is because different pressure distributions can lead to the same global aerodynamic force. For this reason, in recent years, a great deal of effort has been put into measuring pressure distributions on sails with the aim of validating numerical programs (Viola et al, 2011).

Using flexible sails in wind tunnel tests allows different trims to be investigated. The deformation of the mast should be correctly modelled because it has a significant affect on the sail shape and on the sail position with respect of the longitudinal boat axis. Wind tunnel tests are usually performed at wind speeds between 2 m/s and 5 m/s. In wind tunnels with large test sections, the model-scale is of the order of 1/10 of full-scale. As a consequence, in order to achieve the full-scale Reynolds number, the wind tunnel wind speed should be 10 times higher than the full-scale wind speed. Unfortunately, however, the maximum wind tunnel wind speed is usually equal to or less than the

full-scale wind speed. This is because the flexible sails and rigging do not allow testing in high-speed conditions, as they would break!

The attitude of a sail flying high and far from the yacht depends on the ratio between the aerodynamic force developed by the pressure distribution and the gravity force. Therefore, the weight of the model-scale sails should be chosen to achieve the same full-scale ratio between the pressure forces and the gravity force. This criterion leads to the choice of a very light model-scale sailcloth. However, since, the sail is a membrane, such a lightweight cloth would stretch a considerable amount due to the loads it would be subjected to, and this change in shape would alter the aerodynamic loading. Unless the mast is especially bendy, where it needs to bend in the wind tunnel tests, the mast is usually modelled in its deformed "sailing" shape and, often, the sail is cut to its "flying" shape. Thus the sails are tested in the wind tunnel at the correct flying attitude, and thus properly simulate full-scale.

On-water Tests

Both numerical simulations and wind tunnel tests are simplified models of the complex full-scale conditions. When yachts sail, the dynamic movements of the yacht and of the sails are considerable. Moreover, the yacht sails through the turbulent atmospheric boundary layer, which leads to a time dependent flow pattern. The sails are continuously trimmed to take into account the dynamic movements of the yacht, the sails, and the change in the wind speed and direction. All these dynamic effects are modelled with difficulty (and consequently with low accuracy) in CFD, and are normally not modelled in wind tunnels, except in special "dynamic" tests.

Because of the complexity of these dynamic effects, on-water tests are very difficult to perform and suffer from poor repeatability, thus leading to a large uncertainty in the results. Firstly, the fully three-dimensional time dependent wind flow, in which the yacht sails, cannot be measured. For instance, if an anemometer were fixed on the top of the mast to measure the three wind velocity components, the measurement would be affected significantly by the influence of the sail trim. Moreover, even if the flow field was known at a location near the top of the mast, the apparent wind speed and direction changes significantly between the top of the mast and sea level, due to the apparent wind vector being formed by subtracting the yacht velocity off the true wind velocity, and their differences vary considerably between the foot and head of a sail.

Both forces and pressures can be measured onboard. As mentioned above, measuring the pressure distributions is preferable to measuring forces, as it gives a much more complete description of the loading process. It is more difficult to make pressure measurements in downwind conditions than in upwind sailing conditions because the apparent wind speed, and thus the pressure differences measured by the transducer, are lower in the former case. The apparent wind velocity is the vectorial difference between the true wind velocity and the velocity of the yacht. The apparent wind angle AWA is the supplementary angle between the apparent wind velocity and the velocity of the yacht, while the apparent wind speed AWS is the modulus of the apparent wind velocity.

The differential pressure across sails is of the order of magnitude of the dynamic pressure, which is, for instance, about 5.5 Pa for a 3 m/s AWS. To measure a pressure distribution along a sail section, pressure variations smaller than about 1 Pa should be measured. However, 1 Pa pressure change corresponds to a wind speed change as small as 0.3 m/s. Moreover, pressures can change by several pascals per minute due to the incoming atmospheric turbulence. The lower AWS means that these pressure changes from turbulence are superimposed on lower mean values, giving the effect of increased unsteadiness.

Therefore on-water pressure measurements automatically take into account these dynamic effects, which are neglected or poorly modelled by numerical simulations and wind tunnel experiments, but on the other hand, the complexity of the real sailing situation makes the measurements quite complicated to perform, and difficult to interpret because the boundary conditions (i.e. the onset flow conditions) are not known precisely, and so considerable judgement has to be used to decide on the appropriate boundary conditions to be prescribed in any CFD or wind tunnel comparisons.

THE STATE OF THE ART OF PRESSURE MEASUREMENTS ON SAILS

Sail aerodynamics has been widely investigated with numerical modelling. From the 1960s to the end of the last century, most of the computations were performed using potential flow codes. In the past 10 years, RANS codes have become very popular for studying downwind sails. A review of potential flow and RANS applications is presented in Viola, 2009. Over the past few years, only a few LES or DES applications on sails have been published (Wright et al., 2010; Braun & Imas, 2008) but the most important research institutes in sail aerodynamics are all investigating these techniques.

Viola & Flay, 2009, reviews wind tunnel force measurements on downwind sails, while Viola & Flay, 2010a, reviews pressure measurements on sails performed on-the-water and in a wind tunnel. In the following paragraphs, a complementary review of force and pressure full-scale experiments on sails is provided.

Force measurements have been performed more rarely in full-scale than in wind tunnels, due to the associated difficulty and cost. Milgram et al, 1993, at the Massachusetts Institute of Technology (MIT), introduced the innovative concept of an instrumented framework structure located inside the 35-foot yacht *Amphetrete*. The frame connected the rigging to the hull and was instrumented with a 6-component balance that measured the aerodynamic forces in equilibrium with the hydrodynamic forces. Masuyama & Fukasawa, 1997, at the Kanazawa Institute of Technology, developed a similar concept on the yacht *Fujin*. These two papers are mainly oriented towards investigating the aerodynamics of yachts. Conversely, the research described by Hochkirch and Brandt, 1999, at the Berlin University was mainly focused on the hydrodynamics of yachts. They applied a similar "space-frame structure" concept to the 33-foot yacht *Dyna*, as well as having an additional anemometer, and were able to measure the hydrodynamic forces on the yacht appendages.

Full-scale pressure measurements were performed for the first time by Warner and Ober, 1925, at the Massachusetts Institute of Technology (the tests were performed between 1915 and 1921). The authors used U-tube pressure manometers on the S-class yacht *Papoose*. Much later, Flay and Miller, 2006, reported the lessons learned by the Yacht Research Unit (YRU) of the University of Auckland in measuring pressures on the sails of the Farr1020-class yacht *Shokran*. The first pressure distribution with a large number of pressure taps (25 per side) was presented the same year by Puddu et al., 2006, from the University of Cagliari, Sardinia. The authors measured the pressures on the mainsail of a Tornado-class catamaran. Graves et al., 2008, measured the pressures on the mainsail of a IACC-class yacht, but only 5 pressure taps were used. The first modern pressure measurements (after Warner

and Ober in 1925) on headsails was recently performed by Viola & Flay, 2010b. The authors measured pressure distributions on the mainsail and the genoa of the 24-foot yacht *Aurelie*, designed by Sparkman & Stephens.

As far as is known by the authors, full-scale pressure distribution on downwind sails have never been published. The present paper presents the first pressure measurements on an asymmetric spinnaker. The measurements were performed on a 1/3rd-scale sail, which was designed for a 90-foot America's Cup class (AC33) yacht. The sail was tested on a 25-foot Platu25-class yacht.

METHOD

The Sails

The America's Cup is the oldest trophy and richest prize in sport. It has been sailed at irregular intervals every few years since 1852. In the previous few decades, the challenger which races against the defender of the trophy has been selected by winning the Louis Vuitton Cup in the challenger-series. The defender has the privilege of choosing the yacht class rule. In late 2008 and early 2009, it was not clear which yacht class would be used in the 34th America's Cup, and when and where the race would be held. Emirates Team New Zealand, the winner of the previous Louis Vuitton Cup, was investigating the design of the most likely class for the next event. The YRU, which was Emirates Team New Zealand's Official Scientific Advisor, asked North Sails New Zealand to manufacture a 1/3rd-scale AC33-class asymmetric spinnaker for on-water testing. The luff (leading edge), leach (trailing edge) and foot of the sail were 9.2 m, 8 m and 4.9 m respectively.

The spinnaker was built with 4 horizontal panels, which were sewn together with an overlap of about 100 mm at each joint. The overlapped panels made 3 horizontal pockets where 21 pressure taps per pocket were located, and the pockets were used to contain the tubes. The girths of the sail at ¼, ½ and ¾ of the height between the head and foot of the sail corresponding to the positions of the bottom, mid and top pockets, were measured to be 5.5 m, 5 m and 2.9 m, respectively. On each of them, the measuring holes of the first and last pressure taps were 40 mm from to the luff and the leach respectively. Figure 1 shows a schematic drawing of the pressure taps located along the three overlapping joints.

The pressure taps used were thin plastic frusta with base and top surface diameters of 50 mm and 40 mm, respectively. The frustum height was 5 mm. The pressure taps had a hole in the centre of the top surface which connected to a 2 mm diameter metal tube protruding out the side of the tap, as shown in Figure 2. PVC tubes connected to the pressure taps conveyed the pressures to the transducers located inside the yacht cabin. The tubes from all the pressure taps were threaded to the luff (leading edge of the sail) inside the horizontal pockets and then down to the tack (corner of luff and sail foot) inside an additional vertical pocket.

The pressure distributions were measured on the leeward side while sailing on starboard tack (wind coming from the right-hand-side of the yacht), and on the windward side when sailing on the port tack (wind coming from the left-hand-side of the yacht). No pressure measurements were performed on the mainsail. Future research should aim to measure the pressures on the two sails simultaneously. The mainsail used in the on-water tests was a standard Platu25-class mainsail.

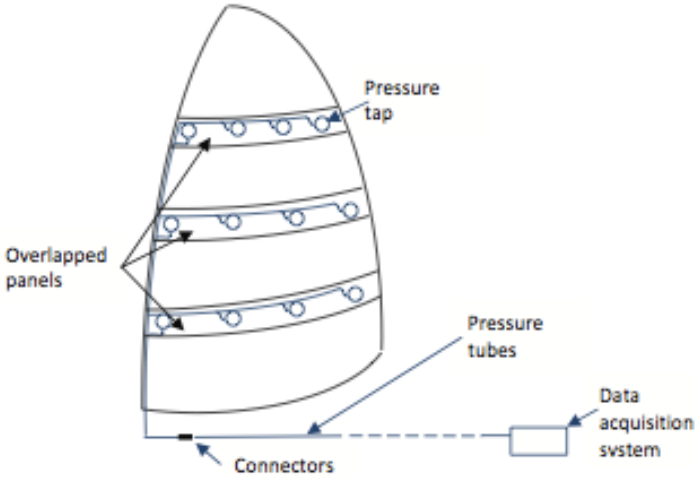

Figure 1: Schematic layout of the pressure-tapped sail (edited from Watier, 2010).

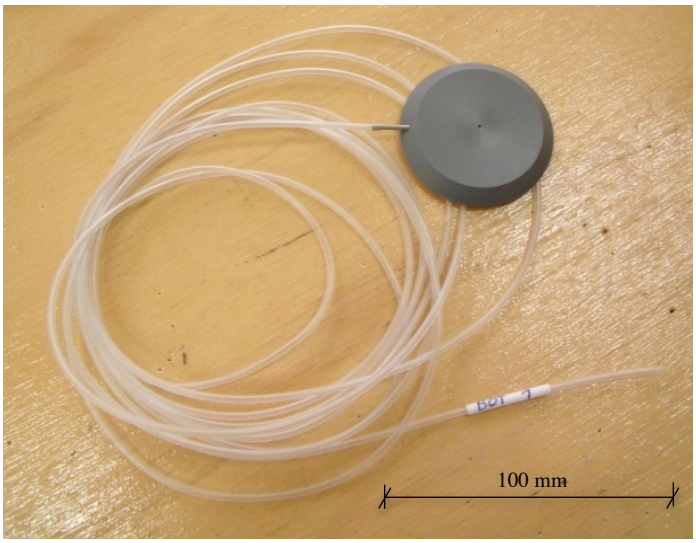

Figure 2: Pressure tap with pressure tube connected.

The Pressure System

The tubes were connected to the transducers, which were well protected inside the cabin. The pressure transducers had a range of ±450 Pa and a resolution of 9.25 mV/Pa with an accuracy better than ±0.5 Pa. Additional details describing the pressure system are provided by Fluck et al., 2010. All the transducers were pneumatically connected to a reference static pressure tube. The tube was 10 m long and the end of the tube was located inside a porous box in a cabinet inside the cabin, which assured that the air inside the box had negligible velocity. The reference static pressure p_∞ was compared with the static pressures measured by Pitot-static probes fixed to a pole on the stern of the boat. The pole was about 2 m high and several Pitot-static probes were fixed onto it. The anemometers were deliberately pointed in different directions. All the static and the total pressures from the Pitot-static probes were connected to the transducers inside the cabin. When the boat was at the wharf, the pressure differences between p_∞ and the static pressures measured on the pole were found to be negligible, as expected. Conversely, the differences between the static pressures were larger while sailing. This was assumed to be due to the influence of the sails on the static pressures measured on the pole. For this reason, the

reference static pressure p_∞ was taken to be that measured inside the cabin, and not by the probes on the pole.

Pressures were acquired at 100 Hz for 90 seconds. High frequency fluctuations would have been damped by the long tubes (up to 20 m long) and hence a higher sampling frequency would have resulted in additional and redundant stored data.

Tests were performed on two different days but all the pressures hereby presented were measured the second day. The pressure transducers were calibrated before testing with the yacht at the dock. In order to take into account thermal effects, about every 20 minutes the tests were interrupted and pressures were measured with the sail inside its bag in the yacht cabin. Thus they were all at the same pressure as the reference pressure. These measured zeros were then subtracted from the signals measured during the actual tests, assuming a linear drift with time.

Pressures were measured using two different approaches. In the first case, pressures were measured with the yacht sailing in the most stable sailing state as possible, with the sails in a fixed state of trim and the yacht on a constant course. Pressures were recorded and averaged over the sampling period. In the second case, pressures were measured while one sail condition was changed at a constant rate. For instance, over 90 s the sail was trimmed in from fully eased to hard in. For these test cases the pressures were averaged in sets of about 15 s duration and the resulting 6 averaged values were used to show the pressure variation with the sail trim.

Measuring the Dynamic Pressure

The dynamic pressure was measured with the Pitot-static probes fixed onto a pole on the stern of the yacht. The pole was mounted on the port side when pressures on the windward side of the sail were measured, and on the starboard side when pressures on the leeward side of the sail were measured. The pole was also inclined at about 20° from the vertical axis of the yacht, so that the Pitot-static probes were always leaning to windward from the yacht. Figure 3 shows the pole supporting the probes while sailing upwind after the tests.

A computational fluid dynamics analysis modelling an AC33-class yacht sailing downwind was performed. It showed that, in the region where the Pitot-static probes were located during the tests, the dynamic pressure is between 0 and 20% higher than in the far field. Conversely, 2 m above the head of the mast, the dynamic pressure is between 20 and 30% lower than in the far field. The consequence of this is that the pressure coefficients that have been presented may be up to 20% lower than they should be. Note that any error in the measurement of q_∞ will only affect the relativity between plots of say “max-eased” with “eased”, since these were recorded at different times, whereas the data across each strip at a particular trim were recorded simultaneously, and a perturbation in q_∞ will affect all results in an identical way.

Initially, a single pivoting Pitot-static probe was mounted on the pole. In a previous experiment (Viola & Flay, 2010b.), where pressures were measured on upwind sails, the wind was able to align the pivoting anemometer used with the wind direction. This setup was not appropriate for the present test, however, because the AWS was not high enough to align the anemometer into the wind. Therefore, three fixed Pitot-static probes aligned in different directions were used. The pressure differences from all three probes were measured at each acquisition, and then the pressure measured by the Pitot-static probe aligned most favourably with the local wind direction (i.e. the one giving the highest reading) was used as the reference dynamic pressure q_∞. In the present paper, q_∞ was between 4 and 40 Pa.

The AWA was measured with the standard on-board yacht instrumentation located at the top of the mast.

Figure 3: Pole supporting the Pitot-static probes (shown while sailing upwind after the tests).

RESULTS AND DISCUSSION

Figure 4 shows the Platu25-class yacht sailing with the pressure-tapped asymmetric spinnaker. In the full-scale AC33-class yacht, the top of the spinnaker is at the same height as the top of the mainsail. Therefore, the measurements were performed with the mainsail lowered (one reef was taken) from the hoist shown in Figure 4, so that the heads of both sails were lined up during the measurements. As a consequence, the lower centre of effort of the mainsail led to a heel angle of approximately 10°, which is lower than that shown in Figure 4.

Three AWAs and several sail trims were measured. The full-scale asymmetric spinnaker was designed to be sailed at about AWA=80° in light air. The Platu25-class yacht does not have a very large righting moment, and therefore an AWA of 80° was a fairly tight angle to be sailed on such a yacht carrying a spinnaker without causing excessive heeling. This is because the lower the AWA, the higher the AWS, and therefore the higher the heeling moment. Two additional (larger) AWAs were tested, namely 120° and 170°.

Figure 4: The yacht and the pressure-tapped sail. The black bands show the locations of the pressure taps. The red bands were used by the VSPARS sail-shape recording system.

The pressure signals were remarkably unsteady for the reasons discussed in the Introduction. It was found that the standard deviations of the pressure time histories were about 50% of their mean values. Indeed, this is not surprising, as the effective turbulence intensity of the AWS is probably in the region of 20 – 30%. In fact, it was not possible to keep a constant sail trim and to sail a constant course. When a gust arrived, the AWS increased and so did the heeling moment. The yacht began heeling and the helmsman reacted immediately to change the course to increase the AWA. The yacht then straightened up and accelerated due to the reduction in hydrodynamic resistance. The increased boat speed led to a lower AWA and the sail then had to be trimmed in. As soon as the gust passed by and the yacht slowed down, the sail became over-trimmed and it had to be eased. Therefore, the AWA and the sail trim were changing continuously. The frequency and the amplitude of the changes in the course and in the sail trim are certainly larger on small yachts such as the Platu25 class, than on large yachts such as the AC33 class, and thus much care has to be taken in transferring the results obtained on a tender keel boat to a more stable large keel boat with a relatively much heavier keel.

The pressure measurements are presented in terms of a pressure coefficient Cp, defined as the difference between the pressures measured by the pressure taps on the sail and the reference static pressure p_∞, measured inside the cabin, divided by the reference dynamic pressure q_∞, measured by the selected Pitot-static probe on the pole. The pressure distributions presented have been smoothed to present general trends. The smoothing was done by fitting polynomials of various orders to the data, where the residual of each was less than 10% of the measured value.

General Pressure Distribution Trends

Pressure distributions on sails can be explained in terms of classical aerodynamic theory for thin airfoils (e.g. see Abbot & Von Doenhoff, 1949). In the mid-height region, the flow direction can be considered mainly in the chord-wise direction. If the local flow at the leading edge is tangent to the sail, then the angle of attack is called the *ideal angle of attack* (Theodorsen, 1931). In this case, the stagnation point is at the leading edge, where the pressure is nearly equal to the stagnation pressure and $Cp \approx 1$. Downstream of the stagnation point, on both the sides of the sail, the pressure drops to lower values. On the leeward side, Cp decreases along the chord until about the maximum depth (draft) of the sail, and then increases again until roughly $Cp \approx 0$ if there is no trailing edge separation, or remains negative if there is trailing edge separation (Katz & Plotkin, 2001). On the windward side, the flow speed is slower and the pressure is nearly constant with positive Cp for most of the chord length. At the trailing edge, the windward Cp decreases to match the leeward-side trailing-edge Cp.

If the leading edge presents a positive angle to the oncoming flow, a leading-edge separation bubble occurs (Katz & Plotkin, 2001). The flow separates from the leeward side of the sail and reattaches again within the first quarter of the chord length. The pressure on the leeward side decreases abruptly near the leading edge, and then increases until approximately the reattachment point. Further downstream, the pressure decreases again due to the sail curvature, and then increases after the maximum sail curvature. This latter pressure increase can lead to trailing edge separation. If trailing edge separation occurs, the pressure recovery is interrupted and the pressure remains nearly constant and equal to the so-called *base pressure*. Figure 5 shows a schematic drawing of the flow field and the corresponding pressure distribution.

As long as the flow does not separate, the higher the angle of attack, the higher the suction near the leading edge. At high angles of attack, the leading edge suction peak is much higher than the cambered-related suction peak, and thus a second peak does not occur. When the flow separates and does not re-attach downstream, the leading edge suction peak decreases. At very high angles of attack, higher than the separation angle, the pressure becomes almost constant and equal to the base pressure.

The stall angle on the mid-section of an asymmetric spinnaker is above 20°. On an equally cambered two-dimensional section, the stall angle would be significantly lower. On three-dimensional sails, the tip vortices take a large amount of flow from the windward side to the leeward side, increasing the pressure on the leeward side. Therefore, the flow is able to reattach downstream at higher angles of attack. More details about the pressure distributions on downwind sails can be found in Viola & Flay 2009 and 2010a.

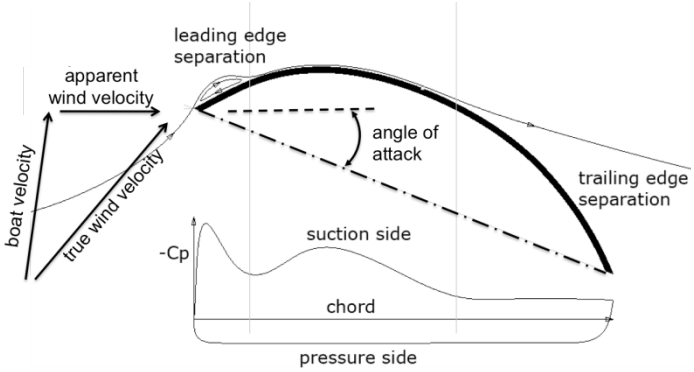

Figure 5: Schematic drawing of the flow field and of the corresponding pressure distribution on a sail section.

Pressure Distributions from Different Trims

Figure 6 shows *Cp's* on the leeward side of the 3 horizontal sections of the asymmetric spinnaker for AWA=120°. *Cp's* are plotted along the curve length for each sail section for 4 different sail trims. The sail is initially eased as much as possible (*max eased* trim in Figure 6). The low angles of attack on the top sections of the sail thus lead to flapping of the leading edge. The pressures on the top section (3/4th of the sail height) show that the sail is trimmed at the *ideal angle of attack*. On the lower sections, a leading edge suction peak occurs, and the *Cp* shows a suction peak within the first quarter of the sail. In the second half of the curve length, trailing edge separation occurs and the *Cp* becomes almost constant.

When the sail is trimmed in just enough to stop the luff from flapping (trim *eased* in Figure 6), a leading edge suction peak occurs on the top section. Sailors would generally consider this to be the optimum trim, i.e. the trim which produces the maximum boat speed. On the middle and bottom sections, the suction peak shows a decrease due to movement of the trailing edge separation point upstream along the curve length. On the top section near the trailing edge, *Cp* decreases down to -3 and shows a symmetrical distribution with respect to the centreline of the sail. These significant changes in pressure distribution across the top section of the sail with trim alterations are very interesting and are discussed in detail in the following paragraphs.

Figure 4 shows a photograph of the Platu 25 sailing at AWA=80°, and it can be seen that the spinnaker pole is close to the forestay. For the results shown in Figure 6 at AWA=120° the spinnaker pole was positioned further aft, and the spinnaker was further around in front of the yacht. It can be seen in Figure 4 that the head of the spinnaker is very narrow, as it is a scaled-down shape designed for an IACC yacht sailing at AWA=80°. Furthermore, as stated earlier, the pressure tests were carried out when the mainsail was reefed so that the heads of the spinnaker and mainsail were aligned, whereas Figure 4 shows the mainsail at full height. According to the Platu 25 class rules, the mainsail girth length at ¾ height is 1380mm. This results in an angle of about 30° at the mainsail head, which is quite low, i.e. it has a rather "pointed" head with not much area near the top. This means that in downwind sailing the mainsail will have much less impact on the behaviour of the spinnaker than a "flat-head" main would. Thus in the following discussion regarding the pressure distributions at the top of the symmetric spinnaker, the effect of the mainsail is ignored, as it is expected to be small.

It is known that a so-called delta-wing, such as used on the supersonic Concord aircraft, produces high lift by having separated flows off both swept-back edges, producing strong spiralling vortices, e.g. see Hummel (2006). These vortices produce strong three-dimensional flow which can cause a wing to exhibit high values of lift coefficient at high angles of attack, as they bring flow downwards onto the central section of such delta wings. For example the 65° delta wing in Hummel (2006) at an angle of attack of 13° has pressure coefficients as low as -2.5 at 20% of the chord downstream of the apex. The highest suction is at the edge, and the lowest suction is in the centre, and is about -0.2. Further downstream the highest suctions move away from the edge, as the pair of vortices grow, and their centres move further inboard from the edges. Such behaviour is not confined to high speed low turbulence aerodynamic flows. Conical vortices resulting in separated flows with low pressures have also been observed above the roofs of buildings emanating from a corner, when the wind is at an oblique angle to the edge discontinuity, e.g. see Ginger and Letchford, 1993.

It has been observed that sails can also exhibit such "delta-wing-type" behaviour (Bethwaite, 2003). Bethwaite states "The head of a spinnaker which is trimmed to float more horizontally than vertically at its head can and should develop these roll-over vortices."

The authors believe that the pressure distributions shown at the ¾ height section of the spinnaker in Figure 6 for AWA=120° for the trims of *eased* and *tight* are exhibiting such delta-wing characteristics, and that this is the first time they have been measured on a yacht sail. The apparent wind direction for these measurements would have been aligned approximately with the bisector of the apex (head) of the spinnaker. This kind of pressure distribution is expected to be caused by flow that was separating off both sides of this "delta-wing-like" spinnaker head shape, and thus producing a pair of strong vortices which cause the low pressures at the sail edges. At lower heights the orientation of the spinnaker becomes more vertical and the angle would have been too large to allow these vortices to remain attached to the upper surface, and so they would have left the sail surface, which is why the pressure distributions are more conventional at lower spinnaker heights. Also, the AWA changes with height, giving an onset flow to the sail which is more aft near the head, and more on-the-beam at the foot. This effectively changes the angle of attack with height, bringing the flow onto the spinnaker leading edge (luff) at the lower heights.

At the ¾ height section, the "max-eased" trim would have allowed the flow at the head to come onto the sail more along the luff, thus enabling the sail to work in a more conventional manner at its ideal angle of attack as mentioned previously. In the "max tight" trim the spinnaker head flattens and takes up a more vertically orientated setting, so that the separated flow is unable to generate vortices that remain along the lee surface, and so the spinnaker shows the conventional uniform low pressures that are found in the disturbed wake behind bluff bodies.

On the windward side (Figure 7), *Cp* is almost independent of the sail trim and, therefore, only *Cp* measured at the optimum trim is shown. Along the chord length, *Cp* decreases only near the trailing edge, where it is adjusting to match the *Cp* on the leeward side. Because the pressure tap closest to the trailing edge was about 100 mm from the trailing edge, the last measured *Cp* on the leeward side is not equal to the last measured *Cp* on the windward side.

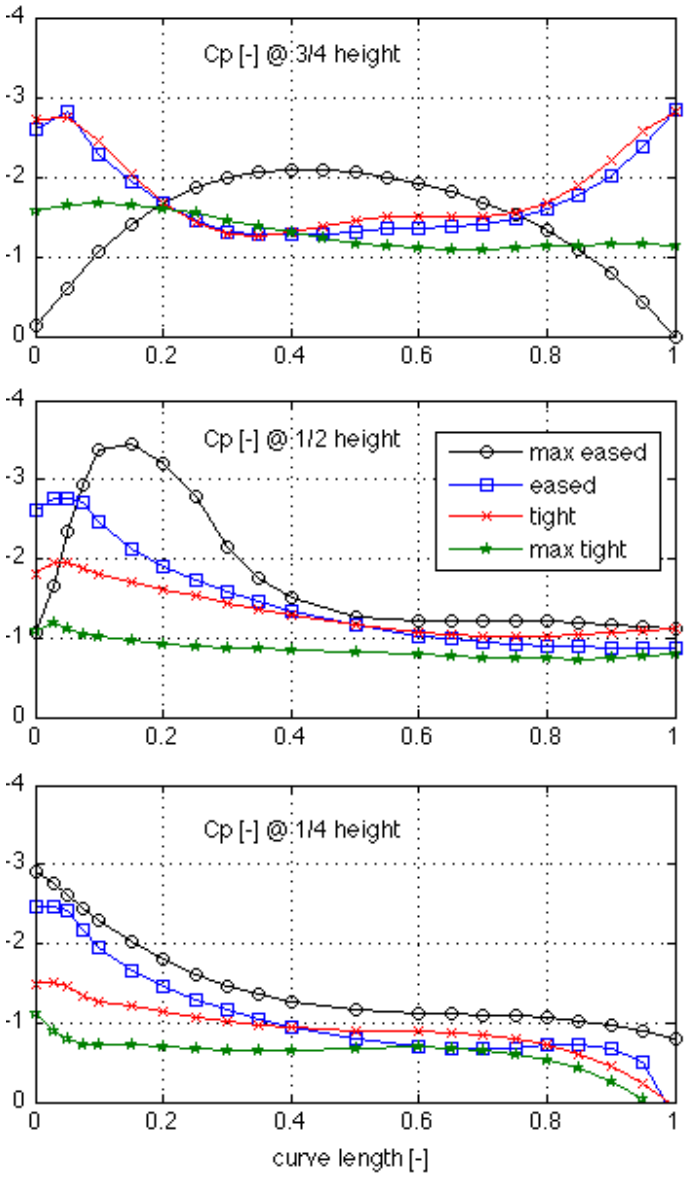

Figure 6: Leeward *Cp* on the 3 sail sections for 4 sail trims.

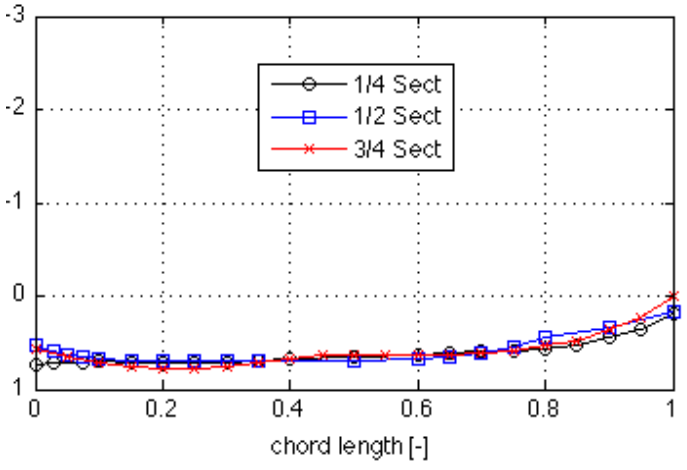

Figure 7: Windward *Cp* on the 3 sail sections.

Pressure Distributions for different AWAs

Figure 8 shows *Cp's* on the leeward side of the 3 horizontal sections of the asymmetric spinnaker for apparent wind angles of 80°, 120° and 170°. The sail was re-trimmed to the optimum trim at each AWA. On the top section, when sailing at AWA=120°, the *Cp* shows the delta-wing-like trailing edge suction. It should be noted that this trailing edge suction does not occur at AWA=80° because for this apparent wind angle the wind is onto the spinnaker luff. At AWA=170° the wind is almost from directly aft, with the spinnaker in front, and the top section of the sail is behaving as a flat plate with a disturbed wake flow resulting in uniform pressure distribution.

Figure 8 shows that the sail can be trimmed at AWA=80° and AWA=120° to achieve a high suction on the entire leeward side of the sail. Conversely, when the AWA is increased further, the sail cannot be eased sufficiently and stall occurs. Along each section, the pressure was observed to oscillate around a nearly constant mean value. The integral of *Cp* along the curve length represents most of the aerodynamic force due to the sail. Figure 8 thus indicates that the aerodynamic force is decreased when stall occurs.

The *Cp's* on the windward side are not presented here because they do not show any significant differences from the *Cp* trends evident in Figure 7.

Full-scale and Wind-tunnel comparison

Figure 9 shows *Cp's* on the leeward side of the 3 horizontal sections of the asymmetric spinnaker, measured on-the-water and in the wind tunnel. *Cp's* were measured on-the-water for the optimum trim at AWA=80°. Wind-tunnel measurements were performed with a 1/15th model-scale flexible sail at the optimum trim at AWA=70°. A detailed description of the wind tunnel measurements can be found in Viola & Flay 2009, and Viola & Flay 2010a.

Figure 9 shows good agreement and similar trends between the *Cp's* measured in full-scale and in the wind tunnel. The *Cp's* measured in full-scale show only one suction peak near the leading edge. Conversely, the *Cp's* measured in the wind tunnel show two suction peaks, the first one being near the leading edge and the second one being near 25% of the curve length. When the angle of attack is increased, which can be due to a tighter trim or to a higher AWA, it has been observed that the leading edge suction peak is increased while the curvature-related suction peak is decreased. Therefore, the differences between the full-scale and the wind-tunnel pressure distributions in Figure 9 suggest that the three sail sections tested in full-scale experienced higher angles of attack than the three sail sections tested in the wind tunnel. In fact, as shown by Viola & Flay, 2010a, different AWAs lead to small differences in the pressure distributions, while larger differences are measured for different trims. A tighter trim is thought to have been used in the full-scale measurements due to having to trim in the unsteady wind conditions. Conversely, the stationary wind conditions and fixed yacht model attitude in the wind tunnel allowed a more eased trim to be used.

Also, it is known that the pressure recovery between the two suction peaks is correlated with the reattachment of the laminar separation bubble. Therefore the differences between the full-scale and wind-tunnel pressure distributions could be due to the absence of the laminar separation bubble during the full-scale experiment. It should be noted that the wind tunnel tests were carried out in uniform untwisted flow, with a lower turbulence intensity (about 3%) than in full-scale

(estimated to be about 20%). Hence the formation of a leading edge separation bubble would be more likely in the wind tunnel with its lower turbulence intensity, and also at the lower Reynolds number, which is about 1/10th of that at full-scale. However, the authors consider that it is more likely that the differences in pressure distributions are due to different sail trims, rather than to Reynolds number effects or to different turbulence characteristics of the flows.

Note also, that as stated above, the full-scale data were smoothed by fitting polynomials of various orders to the data, and this may have inadvertently smoothed out some of the variations that are evident in the wind tunnel data, which were not smoothed in this manner, since these results were much less variable.

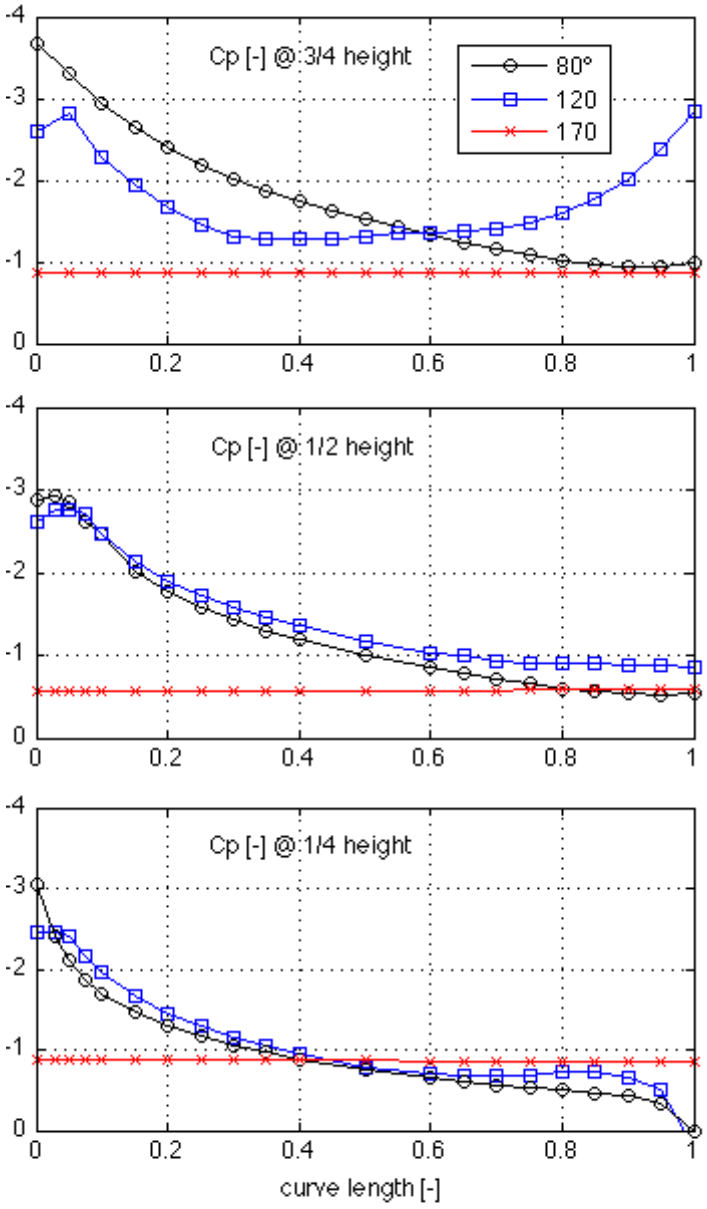

Figure 8: Leeward *Cp* on the 3 sail sections for AWAs of 80°, 120° and 170°.

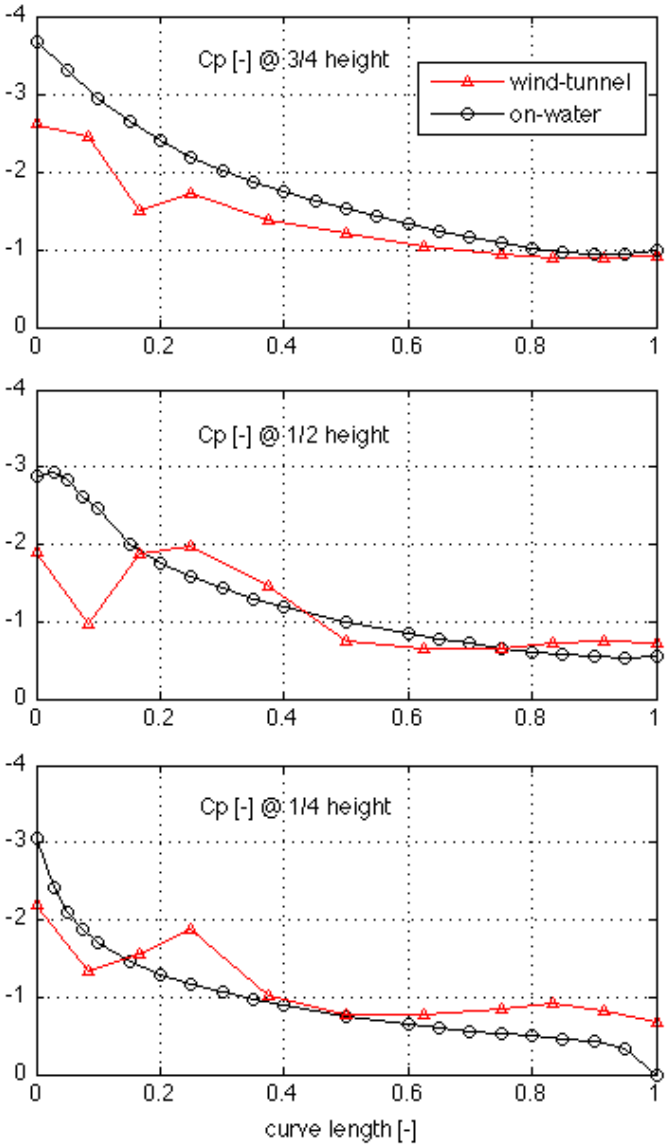

Figure 9: Wind-tunnel and on-water leeward *Cp's* on the 3 sail sections for AWA = 70° and 80°, respectively.

ACKNOWLEDGMENTS

The authors wish to acknowledge the support of the staff and students in the Yacht Research Unit, and in particular, the authors are grateful to Mr. Baptiste Watier and Mr. Etienne Gauvain for their passion and support in managing and performing the on-water and wind tunnel experiments, and Mr David Le Pelley for his helpful advice. The authors also acknowledge the contribution of Dr Nick Velychko in building and supporting the multi-channel pressure system.

CONCLUSIONS

Pressure distributions on sails have been measured only rarely. In particular, on-water pressure measurements have been performed only in upwind sailing conditions. As far as known by the authors, the present paper presents the first full-scale pressure measurements on sails flown in downwind sailing conditions. While numerical modelling and wind tunnel experiments neglect or model relatively poorly the unsteadiness of the wind, the movement of the sails and the yacht, on-water sail tests automatically take them into account.

Pressures were measured using 63 pressure taps distributed along three horizontal sections at 1/4th, 1/2nd and 3/4th of the sail height, on an asymmetric spinnaker. The sail was designed for Emirates Team New Zealand, a possible challenger for the 34th America's Cup, when it was expected to be sailed with AC33-class yachts. Pressure distributions were measured for several sail trims and 3 apparent wind angles (AWAs) on both the leeward and windward sides of the sail.

The main conclusions that can be drawn from the experiments are summarised below.

Pressure Distributions for different TRIMS

- For the optimum sail trims, the *Cp* on the leeward side of the sail near the leading edge has a suction peak between *Cp* = -3 and *Cp* = -4, and downstream, *Cp* increases monotonically.
- On the windward side, *Cp* is almost constant and is slightly less than 1. *Cp* decreases near the trailing edge to match the leeward-side trailing-edge suction.
- In some trim conditions, the suction increases towards the trailing edge on the top leeward section only. It is argued that this is evidence of delta-wing-like vortex formation on the top section of the spinnaker.
- Trimming-in the sail causes the leading edge suction to decrease due to trailing edge separation, until *Cp* becomes almost constant and equal to –1 when stall occurs.

Pressure Distributions for different AWAs

- Almost the same pressure distribution is achieved by re-trimming the sail for AWA=80° and AWA=120°. Conversely, at higher AWAs it was not possible to ease the sail enough and stall occurred. Therefore, *Cp* is almost constant and equal to – 1.
- On the windward side, *Cp* is almost constant at each chord-wise position, between 0 and 1, and decreases near the trailing edge to match the leeward-side trailing-edge suction.

Full-scale and Wind-tunnel comparison

- The full-scale and wind tunnel pressure measurements showed very good agreement in their trends.
- The pressure recovery on the lee side of a spinnaker is related to the leading edge reattachment mechanism. A second suction peak was visible in the first quarter of the curve length for the wind tunnel-measurements, but in the full-scale measurements any leading edge bubble was very small, and so the pressure distribution did not have a second peak, and the suction decreased monotonically towards the trailing edge.

REFERENCES

ABBOTT I.H. & VON DOENHOFF A.E. (1949). "Theory of Wing Sections", *Dover Publications Inc*., New York.

BETHWAITE, F., (2003) "High Performance Sailing", Publ By Adlard Coles Nautical, London.

BRAUN J.B. AND IMAS L. (2008). "High Fidelity CFD Simulations in Racing Yacht Aerodynamic Analysis", *in the proceedings of The 3rd High Performance Sailing Yacht Conference (HPYDC3)*, 2nd-4th December, pp. 168-175, Auckland, New Zealand.

FLAY R.G.J. & MILLAR S. (2006). "Experimental Consideration Concerning Measurements in Sails: Wind Tunnel and Full Scale", *in the proceedings of The 2nd High Performance Yacht Design Conference (HPYDC2)*, February 14th-16th, Auckland, New Zealand.

FLUCK M., GERHARDT F.C., PILATE J. AND FLAY R.G.J. (2010). "Comparison of Potential Flow Based and Measured Pressure Distributions Over Upwind Sails", *Journal of Aircraft,* Vol 47, No. 6, pp 2174-2177.

GAVES W., BARBERA T., BROUN J.B., IMAS L. (2008). "Measurements and Simulation of Pressure Distribution on Full Size Scales", *in the proceedings of The 3rd High Performance Yacht Design Conference (HPYDC3)*, December 2nd-4th, Auckland, New Zealand.

GINGER J.D., LETCHFORD C.W., (1993) "Characteristics of large pressures in regions of flow separation", *Journal of Wind Engineering and Industrial Aerodynamics,* Vol 49, No. 1-3, pp 301-310.

HOCHKIRCH K. & BRANDT H. (1999). "Full-Scale Hydrodynamic Force Measurement on the Berlin Sailing Dynamometer", *in the proceedings of The 14th Chesapeake Sailing Yacht Symposium (14CSYS), SNAME,* pp. 33-44, 30th January, Annapolis, USA.

HUMMEL, D. (2006) "The Second International Vortex Flow Experiment (VFE-2): Objectives and First Results*", in the proceedings of the Institution of Mechanical Engineers, Part G: Journal of Aerospace Engineering,* June 1, Vol. 220, 6: pp. 559-568.

KATZ J. & PLOTKIN A. (2001). "Low-Speed Aerodynamics". *Cambridge University Press*, UK.

MASUYAMA Y. & FUKASAWA T. (1997). "Full-Scale Measurements of Sail force and Validation of Numerical Calculation Method", *in the proceedings of The 13th Chesapeake Sailing Yacht Symposium (13CSYS), SNAME*, pp. 23-36, 25th January, Annapolis, USA.

MILGRAM J.H., PETERS D.B., ECKHOUSE D.N. (1993). "Modeling IACC Sail Forces by Combining Measurements with CFD", *in the proceedings of The 11th Chesapeake Sailing Yacht Symposium (11CSYS), SNAME*, pp. 65-73, 29th-30th January, Annapolis, USA.

PUDDU P., ERRIU N., NURZIA F., PISTIDDA A., MURA A. (2006). "Full Scale Investigation of One-Design Class Catamaran Sails", *in the proceeding of The 2nd High Performance Yacht Design Conference (HPYDC2),* February 14th-16th, Auckland, New Zealand.

THEODORSEN T. (1931). "On the Theory of Wing Sections with Particular Reference to the Lift Distribution", *NACA Report, no 383.*

VIOLA I.M. (2009). "Downwind Sail Aerodynamics: a CFD Investigation with High Grid Resolution", *Ocean Engineering, vol. 36, issues 12-13,* pp. 974-984.

VIOLA I.M. & FLAY R.G.J. (2009). "Force and Pressure Investigation of Modern Asymmetric Spinnakers", *International Journal of Small Craft Technology, Trans. RINA*, vol. 151, part B2, pp. 31-40, 2009, DOI: 10.3940/rina.ijsct.2009.b2.98. Discussion in *Trans. RINA*, vol. 152, part B1, pp. 51-53.

VIOLA I.M. & FLAY R.G.J. (2010a). "Pressure Distribution on Modern Asymmetric Spinnakers", *International Journal of Small Craft Technology, RINA,* Vol. 152, part B1, pp. 41-50.

VIOLA I.M. & FLAY R.G.J. (2010b). "Full-scale Pressure Measurements on a Sparkman & Stephens 24-foot Sailing Yacht", *Journal of Wind Engineering and Industrial Aerodynamics,* Vol 98, No. 12, pp 800-807.

VIOLA I.M., PILATE J., FLAY R.G.J. (2011). "Upwind Sail Aerodynamics: a Pressure Distribution Database for the Validation of Numerical Codes", *International Journal of Small Craft Technology* Vol. 153, part B1, pp. 47-58.

VIOLA I.M., PONZINI R. (2011). "A CFD Investigation with High-Resolution Grids of Downwind Sail Aerodynamics", *in the proceedings of Developments in Marine CFD, RINA*, 23rd-24th March, London, UK.

WARNER E.P. & OBER S. (1925). "The aerodynamics of Yacht Sails", *in the proceedings of The 3rd General Meeting of the Society of Naval Architects and Marine Engineers,* 12th-13th November, New York, USA.

WATIER P.B. (2010). "Comparison of Full-Scale and Model-Scale Measurements of the Aerodynamics of an Asymmetric Spinnaker", *MEng Thesis, DTU Mechanical Engineering, Technical University of Denmark*, Denmark, and Yacht Research Unit Report, The University of Auckland, New Zealand

WRIGHT A., CLAUGHTON A., PATON J., LEWIS R. (2010). "Offwind Sail Performance, Prediction and Optimisation", *in the proceedings of The 2nd International Conference on Innovation in High Performance Sailing Yachts (INNOV'SAIL)*, 30th June – 1st July, Lorient, France.